Title: On the vertices of Lambda polytopes

Speakers: Cihan Okay

Series: Perimeter Institute Quantum Discussions

Date: January 18, 2023 - 11:00 AM

URL: https://pirsa.org/23010105

Abstract: Classical simulation algorithms provide a rigorous ground for investigating quantum resources responsible for quantum speedup. In my talk, I will consider one such algorithm provided by Lambda polytopes. These polytopes are defined to be the polar dual of the stabilizer polytopes and can be used to provide a hidden variable model for finite-dimensional quantum theory. This hidden variable model can be turned into a classical algorithm that can simulate any quantum computation. The efficiency of this algorithm depends on the combinatorial structure of the polytope. In general, which subset of the vertices gives rise to efficient simulation is an open problem. I will describe some of the known classes of vertices and available methods for studying this polytope.

Zoom link: https://pitp.zoom.us/j/95216680309?pwd=aGlIN2NtZVRtczdHcXl5RzgzQTlOdz09

On the vertices of Λ-polytopes

Cihan Okay

Bilkent University

Perimeter Institute - January 2023

Outline

- Motivation and background
- Λ-polytopes
- Closed noncontextual vertices
- Maps between Λ-polytopes
- Decomposing the 2-qubit Λ-polytope[2]

[1] joint with Michael Zurel and Robert Raussendorf
[2] joint with Ho Yiu Chung and Selman Ipek

Quantum computation with magic states

QCM scheme[3]

$$\text{stabilizer subtheory} + \text{“magic state”} = \text{universality}$$

Stabilizer subtheory

(Stabilizer states, Clifford unitaries, Pauli measurements)

Gottesman–Knill theorem: Stabilizer subtheory is efficiently classically simulatable.

An example of a magic state is

$$|T\rangle = T|+\rangle = \frac{|0\rangle + e^{\pi i/4}|1\rangle}{\sqrt{2}}$$

[3] Bravyi and Kitaev 2005.

Odd local dimension

Quantum computation with magic states can have quantum speedup only if the Wigner function of the magic state is negative[4].

Quantum contextuality is a necessary resource for universal quantum computation[5].

A multiqudit quantum state is contextual with respect to Pauli measurements if and only if its Wigner function is negative[6].

---

[4] Veitch et al. 2012.
[5] Howard et al. 2014.
[6] Delfosse et al. 2017.

Wigner functions for d odd

Wigner function of ρ is a quasi-probability distribution $W_\rho : E_n \to \mathbb{R}$ over the phase space $E_n = (\mathbb{Z}_d)^{2n}$.

Properties:

(i) Clifford covariance: For any Clifford unitary U we have

$$W_{U\rho U^\dagger}(a) = W_\rho(S_U(a) + a')$$

where S_U is a symplectic transformation.

(ii) Positivity preservation under measurement: For any Pauli projector Π we have

$$W_\rho(a) \geq 0 \quad \Rightarrow \quad W_{\Pi\rho\Pi}(a) \geq 0$$

If $W_\rho \geq 0$ then QCM can be efficiently classically simulated.

Difficulties for qubits

Any operator basis for the space of n-qubit Hermitian operators fails to be Clifford covariant[7].

Positivity is not preserved under Pauli measurements[8].

Both of the properties above have cohomological underpinnings[9].

The number of classical bits of memory required to simulate contextuality scales quadratically with the number of qubits[10]. Phase space has to be larger than $E_n = (\mathbb{Z}_2)^{2n}$.

---

[7] Zhu 2016.

[8] Raussendorf et al. 2017.

[9] Raussendorf et al. 2021.

[10] Karanjai, Wallman, and Bartlett 2018.

Pauli group

Pauli operators:

$$T_a = i^{a_Z \cdot a_X} Z(a_Z) X(a_X)$$

where $a = (a_Z, a_X) \in E_n = \mathbb{Z}_2^n \times \mathbb{Z}_2^n$ and

$$Z(a_Z) = \bigotimes_{i=1}^{n} Z_i^{(a_Z)_i} \quad \text{and} \quad X(a_X) = \bigotimes_{i=1}^{n} X_i^{(a_X)_i}.$$

Pauli group is defined by $P_n = \{\pm T_a, \pm i T_a | \; a \in E_n\} \subset U((\mathbb{C}^2)^{\otimes n})$.

Clifford group Cl_n is the normalizer (modulo central elements) of P_n:

$$0 \to \mathbb{Z}_2^{2n} \to \mathrm{Cl}_n \to \mathrm{Sp}(\mathbb{Z}_2^{2n}) \to 0$$

Structure of the Pauli group

The commutator of P_n is determined by a symplectic form

$$T_a T_b T_a T_b = (-1)^{[a,b]} I \text{ where } [a,b] = a_Z \cdot b_X + a_X \cdot b_Z$$

E_n together with $[\cdot,\cdot]$ is a symplectic vector space with basis $\{z_1, \cdots, z_n, x_1, \cdots, x_n\}$.

A subspace $I \subset E_n$ is called isotropic if $[a,b] = 0$ for all $a, b \in I$.

Product of Pauli operators:

$$T_a T_b = (-1)^{\beta(a,b)} T_{a+b} \ \forall a, b \text{ with } [a,b] = 0$$

(The function β can be regarded as a 2-cocycle.)

Λ-polytopes

Definition:

$$\Lambda_n = \{X \in \mathrm{Herm}((\mathbb{C}^2)^{\otimes n}) |\ \mathrm{Tr}(X) = 1,\ \mathrm{Tr}(X\Pi_\sigma) \geq 0\ \forall |\sigma\rangle \in S_n\}.$$

The set of vertices is denoted by $\{A_\alpha |\ \alpha \in \mathcal{V}_n\}$.

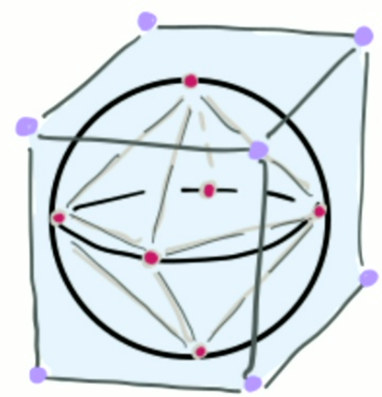

Theorem ([11])

Every n-qubit quantum state ρ can be represented by a probability function $p_\rho : \mathcal{V}_n \longrightarrow \mathbb{R}_{\geq 0}$ where

$$\rho = \sum_{\alpha \in \mathcal{V}_n} p_\rho(\alpha)\, A_\alpha.$$

For any Pauli operator $T_a = \Pi_a^0 - \Pi_a^1$ and vertex A_α the operator $\Pi_a^s A_\alpha \Pi_a^s$, if nonzero, is contained in Λ_n after normalization hence specifies a probability distribution $q_{\alpha,a} : \mathcal{V}_n \times \mathbb{Z}_2 \longrightarrow \mathbb{R}_{\geq 0}$ where

$$\Pi_a^s A_\alpha \Pi_a^s = \sum_{\beta \in \mathcal{V}_n} q_{\alpha,a}(\beta, s)\, A_\beta$$

The Born rule takes the form

$$\mathrm{Tr}(\Pi_a^s \rho) = \sum_{\alpha \in \mathcal{V}_n} p_\rho(\alpha) Q_a(s|\alpha)$$

where $Q_a(s|\alpha) = \sum_{\beta \in \mathcal{V}_n} q_{\alpha,a}(\beta, s)$.

[11] Zurel, Okay, and Raussendorf 2020.

Classical simulation algorithm: Given a quantum state ρ and a sequence $T_{a_1}, \cdots, T_{a_N}$ of Pauli operators representing a computation in the QCM scheme:

1. Sample from the probability distribution p_ρ to obtain a phase space point $\alpha_0 \in \mathcal{V}_n$.
2. For each Pauli measurements T_{a_t}, $a_t \in E_n$, from $t = 1, 2, \cdots, N$, sample from q_{α, a_t} to obtain the new phase space point $\beta \in \mathcal{V}_n$ and measurement outcome s_t.

   Output s_t as the outcome for the measurement of T_{a_t}.

   Update $\alpha_{t-1} \to \alpha_t = \beta$, and $t \to t + 1$.

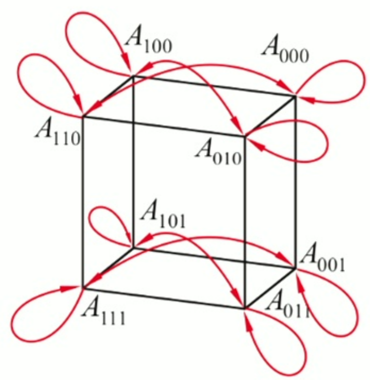

Closed and non-contextual (cnc) sets

A subset $\Omega \subset E_n$ is called

1. closed if $a, b \in \Omega$ with $[a, b] = 0$ implies that $a + b \in \Omega$.
2. non-contextual if it admits a value assignment:

   There exists a function $\gamma : \Omega \to \mathbb{Z}_2$ such that

$$\gamma(a) + \gamma(b) = \beta(a, b) + \gamma(a + b) \quad \forall a, b \in \Omega \text{ with } [a, b] = 0.$$

Ω is called a cnc set if it is both closed and non-contextual.

There is an associated operator

$$A_\Omega^\gamma = \frac{1}{2^n} \sum_{a \in \Omega} (-1)^{\gamma(a)} T_a$$

Cnc-type vertices

The operators A_Ω^γ corresponding to maximal cnc sets (Ω, γ) are vertices of Λ_n:

$$\mathcal{V}_n^{\text{cnc}} = \{A_\Omega^\gamma | \ \Omega \text{ is a maximal cnc set and } \gamma \text{ value assignment}\}$$

The update rule[12] is given by

$$\Pi_a^s A_\Omega^\gamma \Pi_a^s = \begin{cases} \delta_{s,\gamma(a)}\left(\frac{1}{2}A_\Omega^\gamma + \frac{1}{2}A_\Omega^{\gamma+[a,-]}\right) & a \in \Omega \\ \frac{1}{2}A_\Omega^{\gamma \times s} & a \notin \Omega. \end{cases}$$

$\Lambda_n^{\text{cnc}} \subset \Lambda_n$: the convex hull of $\mathcal{V}_n^{\text{cnc}}$.

[12] Raussendorf et al. 2020.

The region of efficient classical simulation

If ρ can be represented by a probability distribution $p_\rho : \mathcal{V}_n^{\text{cnc}} \to \mathbb{R}_{\geq 0}$ then the classical simulation algorithm is efficient[13].

This region can be extended to a larger subpolytope:

1. There exists a map $\Phi : \Lambda_m \to \Lambda_n$ for $m < n$ sending vertices to vertices.
2. Reduced simulation algorithm.
3. New class of vertices of Λ_2 with update rules.

[13] Raussendorf et al. 2020.

The Φ-map

Theorem ([14])

Given an n-qubit Clifford unitary U and an $(n-m)$-qubit stabilizer state $|\sigma\rangle$ the linear map $\Phi : Herm((\mathbb{C}^2)^{\otimes m}) \to Herm((\mathbb{C}^2)^{\otimes n})$ defined by

$$\Phi(X) = U(X \otimes \Pi_\sigma)U^\dagger$$

satisfies the following properties

1. *Φ is injective.*
2. *If $X \in \Lambda_m$ is a vertex then $\Phi(X) \in \Lambda_n$ is a vertex.*
3. *A vertex $X \in \Lambda_m$ is of cnc type if and only if $\Phi(X) \in \Lambda_n$ is of cnc type.*

[14] Okay, Zurel, and Raussendorf 2021.

Beyond cnc-type vertices

1-qubit: All the vertices of Λ_1 is of cnc-type

$$A_\alpha = \frac{1}{2}(I \pm X \pm Y \pm Z)$$

2-qubits: The number of vertices of Λ_2 is 22320.

There are 8 orbits under the action of the Clifford group Cl_2. Note that $|\mathrm{Cl}_2| = 11520$

Among these orbits 2 of them are of cnc-type:

	II	IX	IY	IZ	XI	XX	XY	XZ	YI	YX	YY	YZ	ZI	ZX	ZY	ZZ
Type 1 :	1	0	-1	-1	0	1	0	0	0	-1	0	0	0	-1	0	0

	II	IX	IY	IZ	XI	XX	XY	XZ	YI	YX	YY	YZ	ZI	ZX	ZY	ZZ
Type 2 :	1	0	-1	0	0	1	0	-1	-1	0	1	0	0	-1	0	-1

Isotropic subspaces of E_2

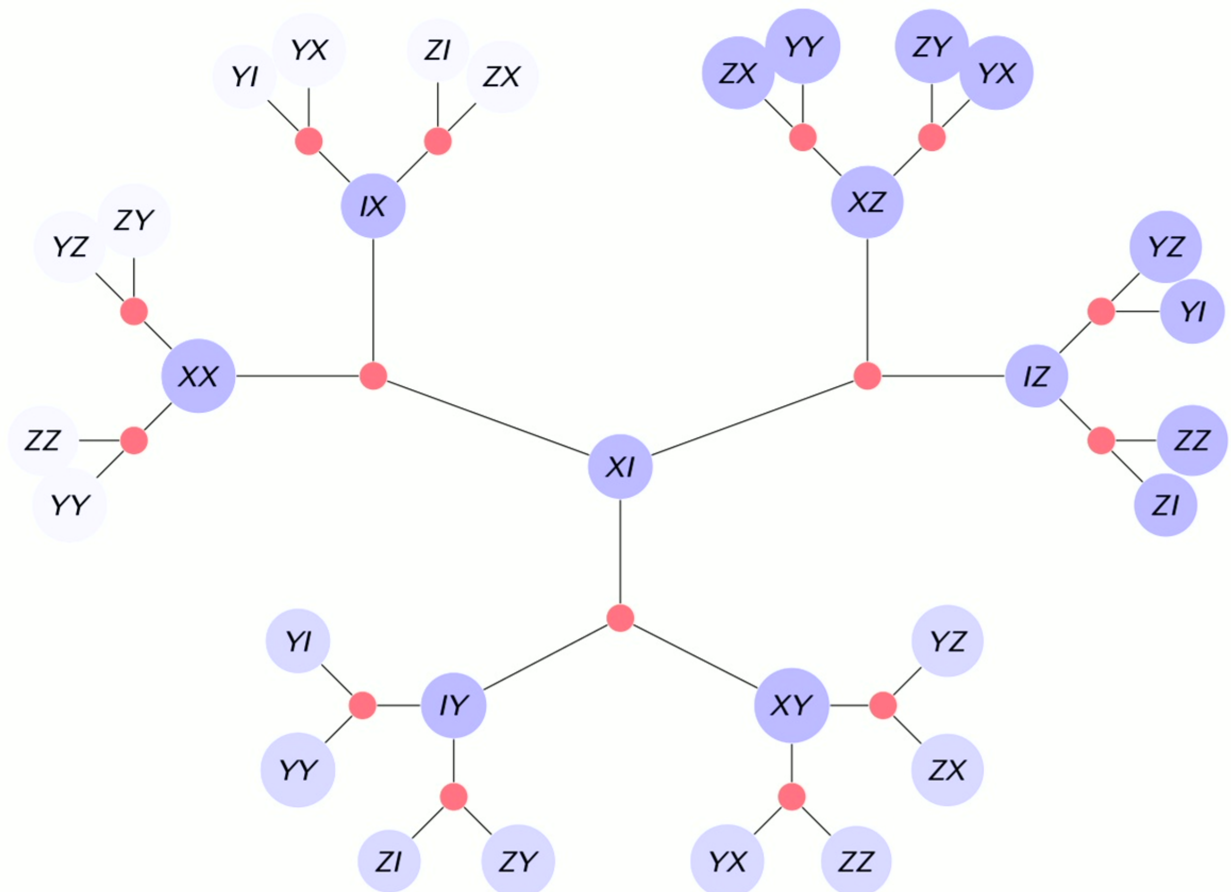

Ω is defined using a collection $\mathcal{C}$ constructed as follows

(i) $\mathcal{C}$ contains I,

(ii) for each $J \in \mathcal{C}$ and $0 \neq a \in J$ exactly one of the two maximal isotropic subspaces distinct from J containing a belongs to $\mathcal{C}$.

Then we define

$$\Omega = E_2 - \hat{\Omega}$$

where $\hat{\Omega} = \left(\bigcup_{J \in \mathcal{C}} J \right) - \{0\}$.

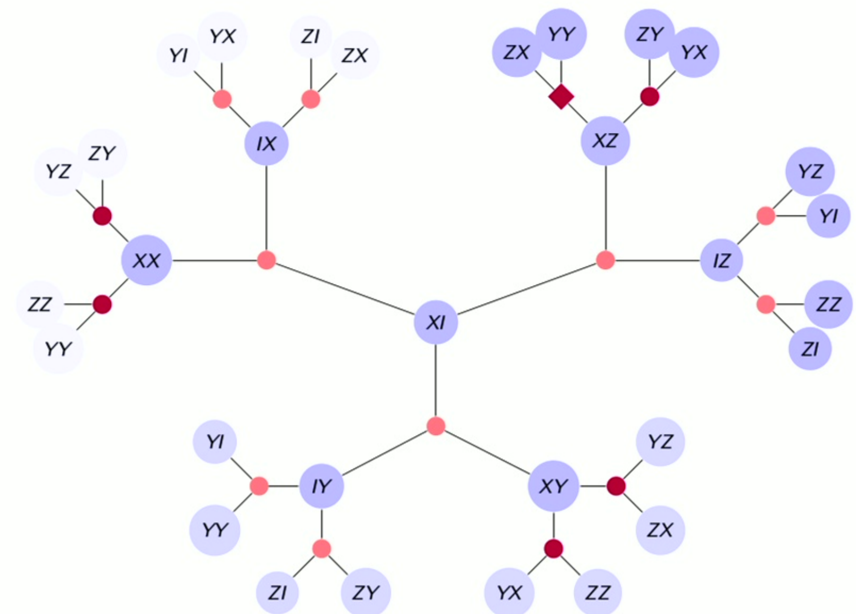

The vertex with coordinates

	II	IX	IY	IZ	XI	XX	XY	XZ	YI	YX	YY	YZ	ZI	ZX	ZY	ZZ
Type 3 :	1	$-\frac{1}{2}$	$-\frac{1}{2}$	$-\frac{1}{2}$	$\frac{1}{2}$	0	0	-1	$-\frac{1}{2}$	0	1	0	$\frac{1}{2}$	-1	0	0

is given by

$$A^{\gamma}_{I,\Omega} = A^{\gamma}_{I} + \frac{1}{4}\left(A^{\gamma'}_{\Omega} - A^{\gamma''}_{\Omega}\right)$$

where

$$I = \langle x_1 + z_2, z_1 + x_2 \rangle \text{ and } \Omega = \{0, x_1, x_1 + z_1, z_1, x_2, x_2 + z_2, z_2\}$$

	II	IX	IY	IZ	XI	XX	XY	XZ	YI	YX	YY	YZ	ZI	ZX	ZY	ZZ
$(-1)^{\gamma}$	1							-1			1			-1		
$(-1)^{\gamma'}$	1	-1	-1	-1	1				-1				1			
$(-1)^{\gamma''}$	1	1	1	1	-1				1				-1			

The update rules

1. $a \in I$ & $a \notin \Omega$

   (1.a) $\gamma(a) \neq s \Rightarrow \Pi^s_a A^\gamma_{I,\Omega} \Pi^s_a = 0$.

   (1.b) $\gamma(a) = s \Rightarrow$

$$\frac{\Pi^s_a A^\gamma_{I,\Omega} \Pi^s_a}{\mathrm{Tr}(A^\gamma_{I,\Omega} \Pi^s_a)} = \frac{2A^{\tilde{\alpha}0}_{\langle a \rangle \perp} + A^{\tilde{\alpha}1}_{\langle a \rangle \perp} + A^{\tilde{\alpha}2}_{\langle a \rangle \perp}}{4}$$

2. $a \notin I$ & $a \in \Omega$

   (2.a) $\tilde{\gamma}'(a) \neq s \Rightarrow$

$$\frac{\Pi^s_a A^\gamma_{I,\Omega} \Pi^s_a}{\mathrm{Tr}(A^\gamma_{I,\Omega} \Pi^s_a)} = A^{\tilde{\alpha}'}_{\langle a \rangle \perp}$$

   (2.b) $\tilde{\gamma}'(a) = s \Rightarrow$

$$\frac{\Pi^s_a A^\gamma_{I,\Omega} \Pi^s_a}{\mathrm{Tr}(A^\gamma_{I,\Omega} \Pi^s_a)} = \frac{2A^{\tilde{\alpha}}_{\langle a \rangle \perp} + A^{\tilde{\alpha}'}_{\langle a \rangle \perp}}{3}$$

3. $a \notin I$ & $a \notin \Omega$

   (3.a) $\tilde{\gamma}'(a) \neq s \Rightarrow$

$$\frac{\Pi^s_a A^\gamma_{I,\Omega} \Pi^s_a}{\mathrm{Tr}(A^\gamma_{I,\Omega} \Pi^s_a)} = \frac{A^{\tilde{\alpha}0}_{\langle a \rangle \perp} + A^{\tilde{\alpha}1}_{\langle a \rangle \perp}}{2}$$

   (3.b) $\tilde{\gamma}'(a) = s \Rightarrow$

$$\frac{\Pi^s_a A^\gamma_{I,\Omega} \Pi^s_a}{\mathrm{Tr}(A^\gamma_{I,\Omega} \Pi^s_a)} = \frac{A^{\tilde{\alpha}0}_{\langle a \rangle \perp} + A^{\tilde{\alpha}1}_{\langle a \rangle \perp}}{2}$$

Extended region of efficient classical simulation

The extended set of vertices consisting of cnc-type and the image of the new class of 2-qubit vertices

$$\mathcal{W}_n = \mathcal{V}_n^{\text{cnc}} \sqcup \{\Phi(A_{I,\Omega}^{\gamma}) | \, (\Omega, I, \gamma)\}$$

where $\Phi : \Lambda_2 \to \Lambda_n$.

If the initial state can be expressed as a probabilistic mixture of the vertices in $\mathcal{W}_n$ then the classical simulation is efficient.

Type 2 :

II	IX	IY	IZ	XI	XX	XY	XZ	YI	YX	YY	YZ	ZI	ZX	ZY	ZZ
1	0	-1	0	0	1	0	-1	-1	0	1	0	0	-1	0	-1

s \ I	XI,IX	XI,IY	XI,IZ	YI,IX	YI,IY	YI,IZ	ZI,IX	ZI,IY	ZI,IZ	XY,YX	XZ,ZX	YZ,ZY	XY,ZX	XZ,YX	XX,YY
11	1/2	0	0	0	0	0	0	0	0	0	0	1/2	0	0	1
-11	0	0	1/2	1/2	0	1/2	1/2	0	1/2	1/2	0	0	0	1/2	0
1-1	0	1/2	1/2	0	0	0	1/2	1/2	1/2	1/2	0	0	1/2	0	0
-1-1	1/2	1/2	0	1/2	1	1/2	0	1/2	0	0	1	1/2	1/2	1/2	0

Type 3 :

II	IX	IY	IZ	XI	XX	XY	XZ	YI	YX	YY	YZ	ZI	ZX	ZY	ZZ
1	$-\frac{1}{2}$	$-\frac{1}{2}$	$-\frac{1}{2}$	$\frac{1}{2}$	0	0	-1	$-\frac{1}{2}$	0	1	0	$\frac{1}{2}$	-1	0	0

s \ I	XI,IX	XI,IY	XI,IZ	YI,IX	YI,IY	YI,IZ	ZI,IX	ZI,IY	ZI,IZ	XY,YX	XZ,ZX	YZ,ZY	XY,ZX	XZ,YX	XX,YY
1 1	1/4	1/4	0	0	1/4	0	0	1/4	1/4	1/4	0	1/4	0	0	1/2
-1 1	0	0	1/4	1/4	0	1/4	1/4	0	0	1/4	0	1/4	0	1/2	1/2
1-1	1/2	1/2	3/4	1/4	0	1/4	3/4	1/2	1/2	1/4	0	1/4	1/2	0	0
-1-1	1/4	1/4	0	1/2	3/4	1/2	0	1/4	1/4	1/4	1	1/4	1/2	1/2	0

Decomposing Λ_2

The local part: Projecting down to local contexts, i.e., those of the form $\langle XI, IX \rangle$ etc, gives an embedding

$$\pi : \Lambda_2 \to \mathsf{NS}_{232}$$

into the nonsignaling polytope of the $(2, 3, 2)$ Bell scenario, i.e., 2 parties, 3 measurements and 2 outcomes.

Alice performs XI, YI or ZI and Bob performs IX, IY or IZ.

The nonlocal part: The remaining contexts, i.e., those of the form $\langle XX, YY \rangle$ etc, can be assembled into a Mermin square linear system with odd parity.

Let MP_1 denote the nonsignaling distributions on the Mermin scenario whose support respects the underlying linear system.

For instance, distributions that come from quantum theory belong to MP_1.

	II	IX	IY	IZ	XI	XX	XY	XZ	YI	YX	YY	YZ	ZI	ZX	ZY	ZZ
Type 2 :	1	0	-1	0	0	1	0	-1	-1	0	1	0	0	-1	0	-1

s \ I	XI,IX	XI,IY	XI,IZ	YI,IX	YI,IY	YI,IZ	ZI,IX	ZI,IY	ZI,IZ	XY,YX	XZ,ZX	YZ,ZY	XY,ZX	XZ,YX	XX,YY
11	1/2	0	0	0	0	0	0	0	0	0	0	1/2	0	0	1
-11	0	0	1/2	1/2	0	1/2	1/2	0	1/2	1/2	0	0	0	1/2	0
1-1	0	1/2	1/2	0	0	0	1/2	1/2	1/2	1/2	0	0	1/2	0	0
-1-1	1/2	1/2	0	1/2	1	1/2	0	1/2	0	0	1	1/2	1/2	1/2	0

	II	IX	IY	IZ	XI	XX	XY	XZ	YI	YX	YY	YZ	ZI	ZX	ZY	ZZ
Type 3 :	1	$-\frac{1}{2}$	$-\frac{1}{2}$	$-\frac{1}{2}$	$\frac{1}{2}$	0	0	-1	$-\frac{1}{2}$	0	1	0	$\frac{1}{2}$	-1	0	0

s \ I	XI,IX	XI,IY	XI,IZ	YI,IX	YI,IY	YI,IZ	ZI,IX	ZI,IY	ZI,IZ	XY,YX	XZ,ZX	YZ,ZY	XY,ZX	XZ,YX	XX,YY
1 1	1/4	1/4	0	0	1/4	0	0	1/4	1/4	1/4	0	1/4	0	0	1/2
-1 1	0	0	1/4	1/4	0	1/4	1/4	0	0	1/4	0	1/4	0	1/2	1/2
1-1	1/2	1/2	3/4	1/4	0	1/4	3/4	1/2	1/2	1/4	0	1/4	1/2	0	0
-1-1	1/4	1/4	0	1/2	3/4	1/2	0	1/4	1/4	1/4	1	1/4	1/2	1/2	0

Marginalizing to nonlocal operators and then extending to nonlocal contexts defines a map

$$\text{ext} : \mathsf{NS}_{232} \to \mathsf{MP}_1^{\mathbb{R}}$$

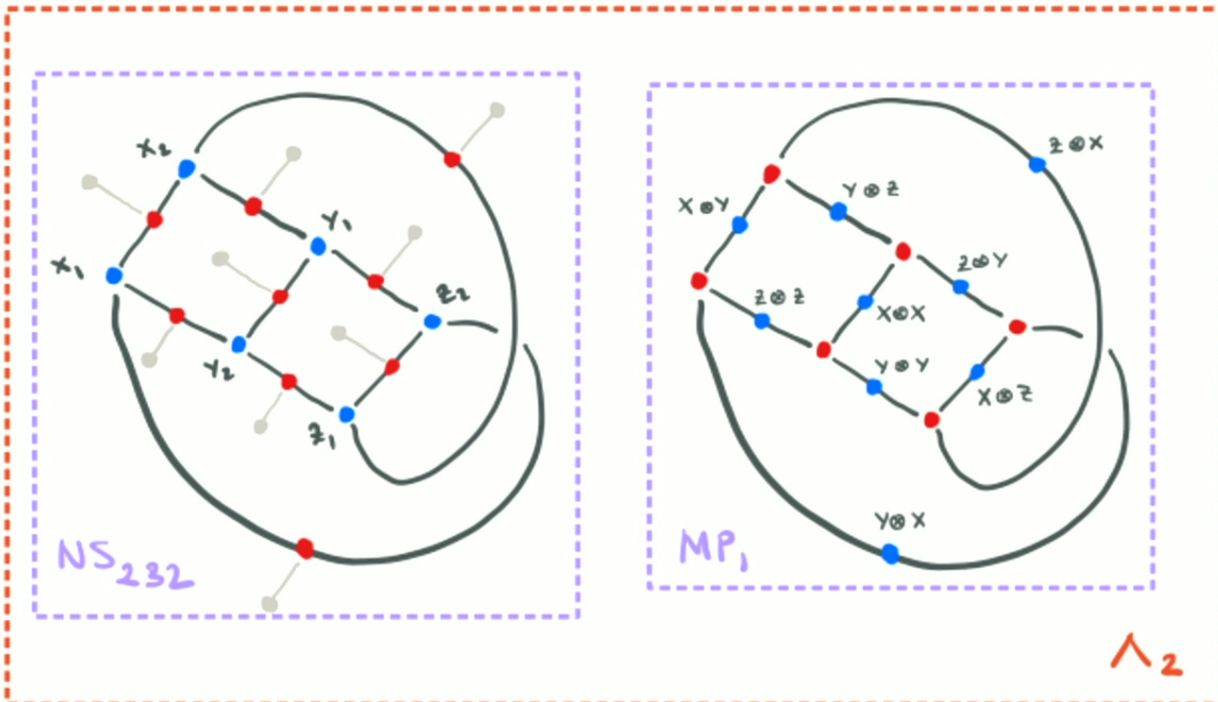

Marginalizing to nonlocal operators and then extending to nonlocal contexts defines a map

$$\text{ext} : \text{NS}_{232} \to \text{MP}_1^{\mathbb{R}}$$

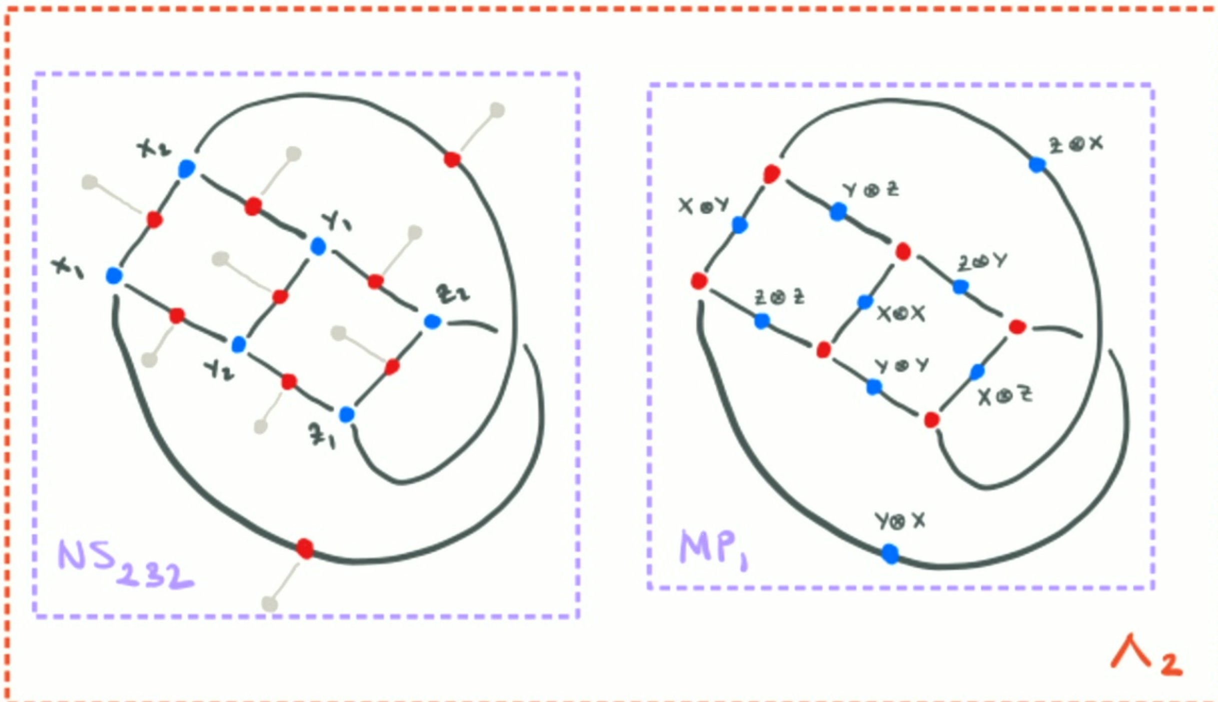

The local vs nonlocal decomposition:

$$\begin{array}{ccc} \Lambda_2 & \overset{\pi}{\hookrightarrow} & \mathrm{NS}_{232} \\ \downarrow & & \downarrow \mathrm{ext} \\ \mathrm{MP}_1 & \hookrightarrow & \mathrm{MP}_1^{\mathbb{R}} \end{array}$$

Λ_2 is precisely the preimage of MP_1 under the ext map.

This gives a decomposition of Λ_2 into two polytopes NS_{232} and MP_1 whose vertices are well-understood.

Vertices of MP_1 are given by maximal nonlocal cnc sets[15].

[15] Okay, Chung, and Ipek 2022.

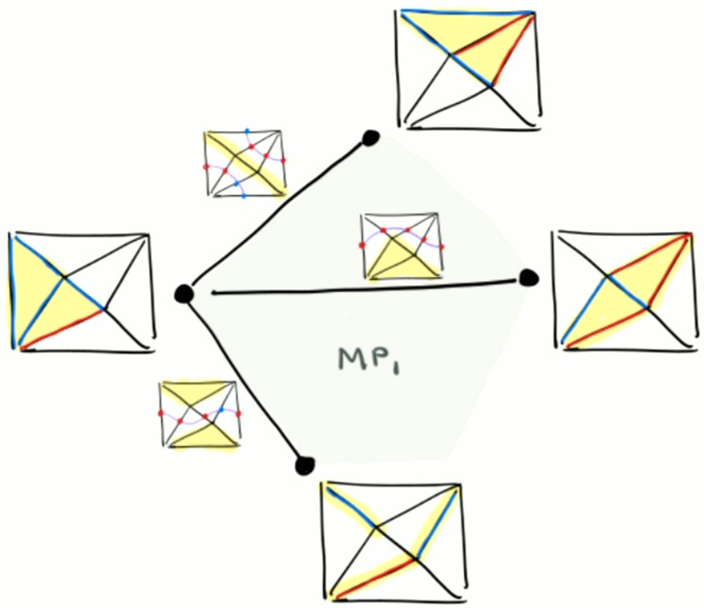
MP1

Connections and open problems

- Classification of vertices of Λ_n.
- Update rules under Pauli measurements.
- The role of symmetries, i.e., the Clifford action.
- Arbitrary local dimensions[16].
- Relation to other polytopes, e.g., nonsignaling.

[16] Zurel et al. 2021.

Thank you for your attention!